Wavelet Analysis for Classification of Multi-source PD Patterns

E. M. Lalitha and L. Satish
Dept. of High Voltage Eng.
Indian Institute of Science, Bangalore, India

ABSTRACT

Multi-resolution signal decomposition (MSD) technique of wavelet transforms has interesting properties of capturing the embedded horizontal, vertical and diagonal variations within an image in a separable form. This feature was exploited to identify individual partial discharge (PD) sources present in multi-source PD patterns, usually encountered during practical PD measurements. Employing the Daubechies wavelet, features were extracted from the third level decomposed and reconstructed horizontal and vertical component images. These features were found to contain the necessary discriminating information corresponding to the individual PD sources. Suitability of these extracted features for classification was further verified using a radial basis function neural network (NN). Successful recognition was achieved, even when the constituent sources produced partially and fully overlapping patterns, thus demonstrating the applicability of the proposed novel approach for the task of multi-source PD classification.

1 INTRODUCTION

DIAGNOSTIC measurements are performed to assess the status of insulation systems in HV power apparatus. This has been a topic of continued interest in the past couple of decades. Presently, there is a greater emphasis in the power industry and amongst utilities to perform on-site, and even on-line diagnostic measurements [1]. This philosophy has been influenced primarily by the increasing use of digital hardware and computers (which afford making such measurements), followed by possibilities of post-processing the gathered data. Among the various diagnostic techniques, partial discharge (PD) measurement is generally considered important, since it is nondestructive, non-intrusive and can qualitatively describe the overall integrity of the insulation system. Use of digital PD equipment is now more or less a standard, a fact recognized even by the forthcoming IEC Standard-60270 [2]. The data gathered from a digital PD detector is popularly referred to as a ϕ-q-n pattern, or PD fingerprint. These patterns contain certain characteristic features that are representative of a particular class, and this criterion has been used widely for recognition of the PD source [3].

In the opinion of the authors, there are basically two outstanding issues associated with the analysis of acquired PD data. The first one is that of effectively storing, handling and subsequently processing the large mass of PD data to perform analysis. Such a situation can be visualized during PD monitoring of power apparatus during its service life. Additionally, it is also well known that insulation behavior is better understood and assessment of its status far more reliable, when PD data gathered under service life conditions, over large intervals of time, is available. Thus arises the necessity of accumulation and processing a large amount of data. A possible solution addressing this issue was presented recently by the authors [4].

The second issue concerns processing the acquired PD data for identification of the PD source. The last decade has seen much research in this area. Various features have been extracted and classification was performed using different pattern recognition methods, with varying degree of success. However, in a majority of these approaches, the presence of only one PD source being active at a given instant, is assumed implicitly.

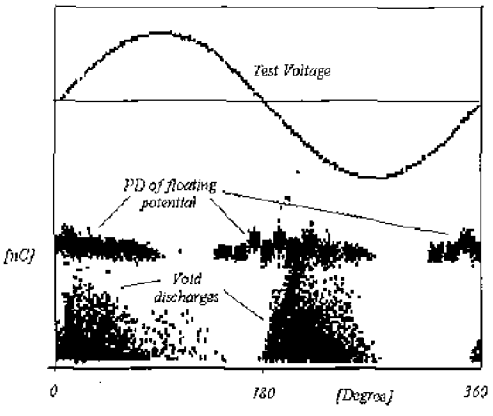

Figure 1. A multi-source PD pattern acquired from a generator stator winding [6].

Unfortunately, the situation encountered during practical PD measurements is far different, and most often, more than one source of PD is active simultaneously; the sources could be internal to the apparatus insulation or may be due to interference. In the latter case, there exist

1070-9878/0/ $3.00 © 2000 IEEE

a few methods like gating/windowing, pulse discrimination and digital filtering, that are employed to suppress its influence. When more than one PD source is simultaneously active, the resultant PD pattern obtained will in a broad sense be the sum of the patterns due to the individual sources. Strictly speaking, the pulse resolution time of the PD detector plays a crucial role in this situation. Given a short pulse resolution time, most of the pulses will be well resolved, and then it would be fair enough to consider the resulting pattern to be a sum of individual PD patterns. This has been verified experimentally [5]. It generally is agreed that identification of the constituent sources in a PD pattern with one or more sources producing overlapping patterns is quite involved. As an example, Figure 1 shows a PD pattern (drawn from [6]) due to singular floating potential and void discharges in a stator winding. The fact that this task is still possible in the above figure is mainly because the pattern contributions due to individual sources are as yet non-overlapping. The recognition task tends to become progressively difficult when the degree of overlap increases along both the magnitude and phase axes. Even for an expert, when presented with such overlapping patterns, it apparently becomes difficult to discriminate and identify the presence of individual sources, despite having a knowledge of the shape of the PD patterns due to individual sources. Since such situations are not uncommon during practical PD measurements, it will be worthwhile to explore newer methods capable of addressing such tasks. This precisely is the aim of this paper.

In recent years, some preliminary investigations have been made for classification of multiple source PD patterns. A stochastic procedure based on mixed Weibull functions applied to PD pulse-height distributions was reported in [7]. A two-parameter Weibull function was observed to be sufficient to characterize the PD pattern of individual sources, while a five-parameter Weibull function was necessary for the mixed patterns. Finally, it was concluded that if one PD phenomena completely or partially superimposes onto the other, identification and separation of the constituents would be virtually impossible [7]. The use of a neural network (NN) for separation of the constituent sources from a two-source PD pattern was examined [8]. It was concluded that the trained NN yielded incorrect results when presented with PD patterns, for which it was not trained. Making a passing reference to this task, Pearson *et al.* used a NN and concluded that, if the contribution of one of the two sources considered is >50%, the NN decides on the source whose percentage in the mix is larger [9]. Such performances are, perhaps due to non-separability of the features (corresponding to constituent sources) being fed to the NN. Separation of constituent PD sources from a two-source pattern was attempted by contour identification of the charge and phase distributions [10]. It was concluded that the superposed patterns can be separated only if there was not much overlap of the two individual patterns. Use of statistical features also have been examined for this task [11], but it was reported that the method is not fully suitable and the necessity for improved methods was highlighted. Thus, from an analysis of the literature, it emerges that the multi-source PD pattern recognition task (in its true sense) as yet is an unresolved issue, and hence the subject of this paper.

In this contribution, the authors address the task of multi-source PD recognition, considering two sources to be simultaneously active and producing partially or fully overlapping PD patterns. A prior knowledge of PD patterns due to individual sources is the only information being assumed to be available. The novel use of wavelet transforms for this task is investigated, in particular multi-resolution signal decomposition (MSD). Results illustrate that even when the two sources produce completely superposed PD patterns, it is still possible to separate the individual PD sources, thus demonstrating the potential of this new method.

The paper is organized as follows. Section 2 deals with a short review of wavelet transforms and multi-resolution signal analysis concepts. The underlying principle of how this method can be adopted to the multi-source PD problem is discussed in Section 3. A brief introduction to digital PD measurements and the pattern database used is presented in Section 4. Details of the proposed scheme, method of feature extraction and a discussion of classification results are presented in Section 5, followed by conclusions and references.

2 WAVELET TRANSFORM AND MSD

The representation and analysis of digital data using wavelets has emerged as a very powerful and popular tool in recent years, with significant successes in areas such as data compression, image and speech processing, remote sensing, medical imaging and so on [12, 13]. The wavelet transform, like the Fourier transform, decomposes a given signal into its frequency components, but differs in providing a non-uniform division of the frequency domain. Unlike the Fourier transform, it provides a local representation in both time and frequency simultaneously. This results from the fact that the analyzing or basis functions in the case of Fourier transform (namely sines and cosines) extend over infinite time, whereas they are compact functions of time in the case of wavelet transforms. Mathematically, the continuous wavelet transform (CWT) of a function $f(t)$ with respect to a mother wavelet $g(t)$ is defined as [12, 13]

$$W_g[f(t)](a,b) = W_g f(a,b) = |a|^{-0.5} \int f(t) g^* \left(\frac{t-b}{a} \right) \quad (1)$$

where a is the scale factor (real, $a \neq 0$), b the translation parameter, and $*$ is the conjugation operator. A mathematical restriction on the choice of $g(t)$, called the admissibility condition, exists. Some examples of popularly used mother wavelet functions are Morlet, Daubechies, Haar, Coifman, *etc.* The choice of the mother wavelet depends on the application and no general rule exists for its selection. The function $W_g f(a,b)$ gives an indication of the contribution of the signal around time b and scale a *i.e.* signal information at different resolutions. However CWT is computationally expensive and also generates much redundant data. To circumvent these drawbacks, an effective implementation applicable to discrete signals, called the discrete wavelet transform (DWT) was formulated using suitable filters, which satisfy certain constraints. An elegant procedure called the multi-resolution signal decomposition (MSD) technique [12] is implemented through this method, which is the primary reason for the widespread use of wavelets.

In DWT the signal is passed through a low-pass filter $\mathbf{G}_A$ (see Figure 2(a)), called the scaling function, and a high-pass filter $\mathbf{H}_A$, called

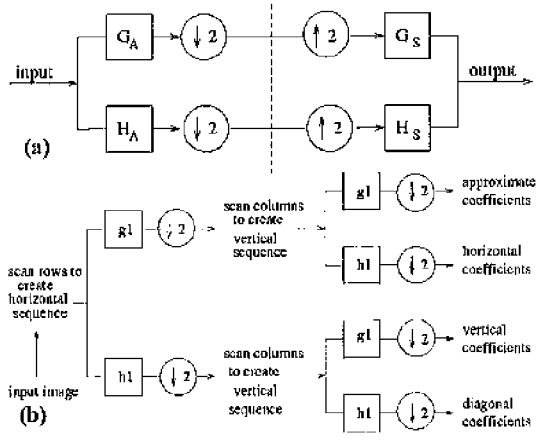

Figure 2. Block diagrams depicting the concepts of MSD (a) single-stage analysis and synthesis (b) single-stage analysis of an image.

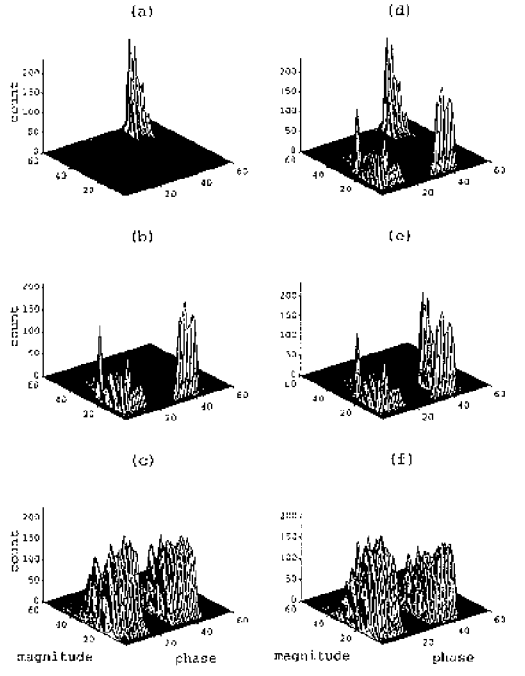

Figure 3. PD patterns of individual and superposed sources (a) single point corona in air, (b) surface discharge, (c) cavity discharge, (d) superposed (a) and (b), (e) superposed (a) and (b) with magnitude shift in (a), (f) superposed (b) and (c).

the mother wavelet, and then each output is downsampled by a factor of two. The output of $\mathbf{G}_A$ (approximate coefficients) are the high-scale (low-frequency) components and output of $\mathbf{H}_A$ (detailed coefficients) are the low-scale (high-frequency) components. The detailed coefficients represent the signal's characteristics and energy at higher frequencies, while the approximate coefficients are a blurred version of the original signal. The decomposition process (analysis stage) can be iterated with successive approximate signal components being decomposed in turn, so that the signal is further divided into many levels of lower resolution components. Thus, it gives information of the signal at different resolutions and this MSD popularized the concept of wavelet analysis. Analogous to the decomposition scheme, the signal coefficients can be reconstructed (synthesis stage) using another set of filters ($\mathbf{G}_S$, $\mathbf{H}_S$) to give the extent of signal present at different scales. The analysis and synthesis filter pairs are inter-related and referred to as quadrature mirror filters. Imposition of certain constraints on these sets of filters ensures a perfect reconstruction. In other words, summing all the reconstructed signal components (obtained at different levels of decomposition) yields the original signal.

For a 2D signal, say an image, the rows and columns are considered separately for decomposition. Figure 2(b) gives the detailed block diagram of single stage decomposition of an image. The horizontal and vertical sequences are separately filtered and subsampled. When the sequences are processed as shown in the Figure, the output of decomposition at every level yields four sub-images, namely one approximate and three detailed coefficients. In the reconstruction process, these coefficients are again upsampled and filtered; for details see [12, 13]. The reconstructed component images are referred to as approximate (A) and detailed horizontal (H), vertical (V), and diagonal (D) images. A blurred version of the input image is represented by A, whereas H, V and D characterize the horizontal, vertical and diagonal variations of the original image respectively. Here also, a sum of all the reconstructed images (corresponding to each level of decomposition) yields the original image.

3 MULTI-SOURCE PD PROBLEM

3.1 AN EXAMPLE

An example highlighting the difficulty encountered in separation of individual PD sources from a multi-source PD pattern is illustrated in Figure 3. Three PD sources *viz.* single point corona in air, surface discharge and cavity discharge are considered and shown in Figures 3(a) (b) and (c), respectively. A 3D view of the patterns is given for purposes of clarity. Figures 3(d), (e) and (f) are the two-source PD patterns obtained by digitally superposing two of the single source PD patterns. In Figure 3(d), which is the result of adding Figures 3(a) and (b), it is seen that the PD pulse clusters of the two sources are non-overlapping. Hence, an expert with some knowledge of the shape of PD patterns from individual sources, can identify the presence of sources by analyzing the phase and magnitude positions of the clusters, together with the extent of spread along each axes.

Usually, in practical PD measurements, pulse clusters of individual PD sources are either partially or completely overlapping. Under such conditions, it is almost impossible to identify, by visual inspection, the presence of different sources. The partial and complete superimposed cases are shown in Figures 3(e) and (f) respectively. Figure 3(e) is the superposition of Figure 3(a) and (b), with a magnitude shift intensionally incorporated into Figure 3(a). The individual pulse cluster information being not clear in Figure 3(e) leads to some uncertainty and thereby causes an ambiguity in recognition. In some cases, phase and magnitude spreads, and also the position of pulse clusters may be similar, leading to a complete overlap. This is evident in Figure 3(f), which is obtained by adding Figures 3(b) and (c). When Figure 3(f) is examined, even with prior information that two sources are present, it is very difficult to discriminate the presence of the sources. The principle of how

wavelet transforms can be used effectively to resolve such recognition tasks, is discussed next.

3.2 UNDERLYING PRINCIPLE

Use of wavelets in analyzing an input signal or image by decomposition of the input and subsequent reconstruction of only those portions that are of interest, assists in improved analysis, since each portion can be analyzed separately. Figure 4(a) shows a completely overlapping multi-source PD pattern (surface discharges and cavity discharges) plotted as a 64 gray-scale image. A three level MSD using the Daubechies wavelet with 56 coefficients was implemented on this image. A reconstruction at the third level yielded four sub-images, namely, the approximate (A), horizontal (H), vertical (V) and diagonal (D) images, and only these are shown in Figures 4(b) to (e).

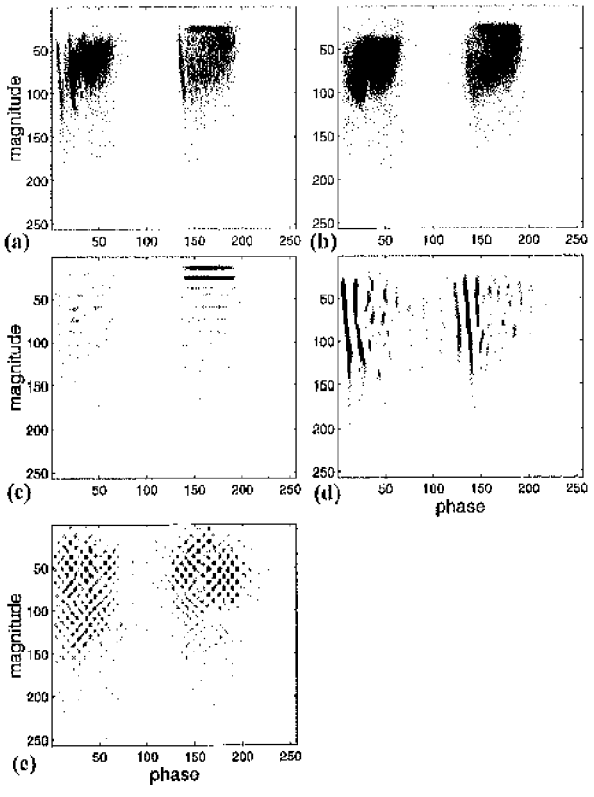

Figure 4. Original and third-level reconstructed images of the superposed PD pattern in Figure 3(f). (a) original (b) approximate (c) horizontal (d) vertical (e) diagonal.

Figure 4(b), the approximate image (A), is a smoothed version of the original image. On visual inspection, it is evident that this image contains no more additional information when compared to the original image. Figure 4(c) represents the horizontal variations and Figure 4(d), the vertical variations embedded in the original. Figure 4(e) shows diagonal variations present in the original, and similar to Figure 4(b), does not seem to contain any specific information pertaining to the two sources. After a considerable amount of study of all the A, V, H and D images, obtained from processing different single and multi-source patterns, it emerges that only the H and V images contained relevant information, that perhaps could aid in separation of the constituent sources present in the input. The basis of choosing H and V image components from among the four sub-images was by visual inspection.

A decision regarding the number of levels of decomposition and the choice of mother wavelet coefficients was made after an extensive examination of all the reconstructed image components at different levels, arising due to different multi-source PD patterns. The studies revealed that a 3-level decomposition-reconstruction using the Daubechies wavelet with 56 coefficients was found to be adequate. Further, restricting analysis to only the third level images turned out to be sufficient for the purposes of the underlying task. Lastly, the ability to provide a separation of features present in the original image into each one of the decomposed components is a fundamental property afforded by the multi-resolution analysis [12]. Explanation on how these H and V images represent features that can lead to discrimination and classification of the individual PD source is explained below with an example.

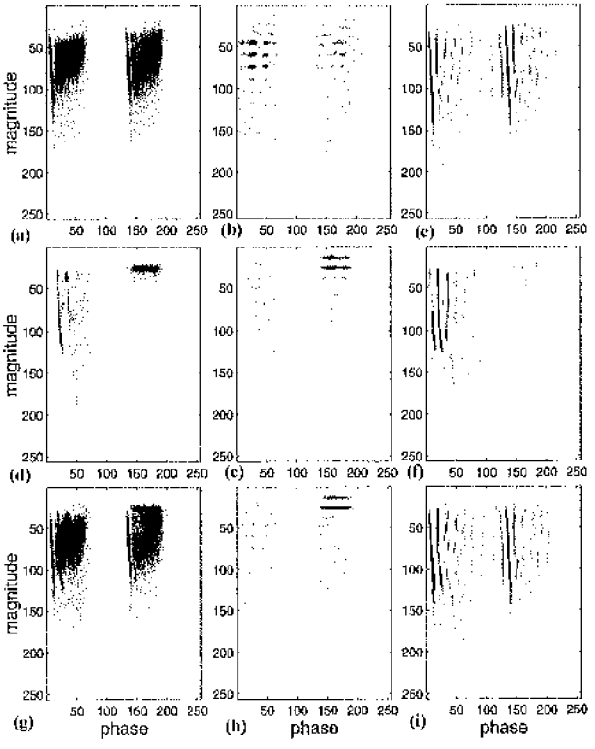

Figure 5. H and V images of individual and superposed PD patterns (a) cavity discharge, (b) H image of (a), (c) V image of (a), (d) surface discharge, (e) H image of (d), (f) V image of (d), (g) (cavity + surface) discharge, (h) H image of (g), (i) V image of (g).

Figures 5(a) and (d) are the patterns due to individual sources (cavity discharges and surface discharges respectively) and Figure 5(g) that due to superposition of these individual sources. Figures 5(b), (e), and (h) are the third level decomposed and reconstructed H images, and Figures 5(c), (f) and (i) are the third level decomposed and reconstructed V images of those shown in Figure 5(a), (d) and (g) respectively. Explanation of the observations is made by considering the first and second half cycles of the sine-wave separately (pixels 1 to 128 and 129 to 256

in the horizontal direction represent the first and second half cycles respectively).

In Figure 5(b), the H components of cavity discharges are not so prominent in both half cycles. In contrast, in Figure 5(e), the presence of dark lines in the horizontal direction clearly indicates that the H component of surface discharges is very prominent in the second half cycle. The H component of the superposed image should thus reflect these properties. Inspection of Figure 5(h) reveals that the H components are less significant in the first half cycle, but are very prominent in the second half cycle, thus revealing the possible presence of surface discharges. Next, consider the V images of the individual and the superposed images in Figure 5(c), (f) and (i) respectively. It is seen that in Figure 5(c), the V component is prominent (indicated by dark vertical lines) in both pulse clusters. In Figure 5(f), the V component is prominent in the first half cycle only. This is indicated by dark vertical lines in the first half cycle. The V image of the superposed case (Figure 5(i)) shows the presence of prominent V components in both the half cycles, indicating the possible presence of cavity discharges. The proposition of only considering the H and V images was confirmed, when similar observations were made, while examining several examples of multi-source PD patterns along with their single source patterns.

To summarize, visual inspection of the H and V images of the multi-source image (Figure 5(h) and (i)) reveals that the salient features which are present in the individual sources, also are present in them, and most importantly, are available in a separable form. The fact that such a separation was possible by this procedure is the underlying principle that was exploited. Additionally, it was also observed that the phase and magnitude positions of the individual sources remain unaltered in Figures 5(h) and (i) respectively, although it is not readily distinguishable in the original image. Very similar observations were seen in the other two cases *viz.* partial and non-overlapping situations. These observations, in general, were found to exist in all the multi-source PD patterns investigated. Salient features are defined and extracted from the H and V components for classification of individual PD sources present in the two-source PD pattern. In this manner, a simple and workable solution is proposed for identifying the individual PD sources present in a given PD pattern.

4 DETAILS OF PD PATTERNS

4.1 BRIEF INTRODUCTION TO PD

PD is a localized breakdown event occurring due to minute defects in insulation structures. These defects are inevitable during manufacture or could develop during the service life of the apparatus, in spite of the best efforts and precautions. PD usually is a pulsive event of very short rise time and relatively longer fall time (at defect sites), and these values depend on the type of insulation. Quantifying of PD in terms of apparent charge is very popular and correlates well to the overall insulation degradation [1].

The digital PD detector is actually an extension of the analog counterpart. It involves digital acquisition of all the individual quasi-integrated pulses (to the extent supported by the hardware) and quantifying each of them by their apparent charge magnitude (q), the corresponding phase angle (ϕ) at which they occur, and their number densities (n) over an interval of time. In other words, the phase and charge axes are divided into bins and the pulses are sorted into these bins, finally yielding the ϕ-q-n pattern. As can be seen from the Figures, PD pulses tend to occur in clusters and, in general, PD patterns from a particular source occupy specific phase positions and spreads. This information is vital for recognition purposes.

4.2 PD PATTERN DATABASE

Three types of PD patterns were considered in this study. They are single point corona, cavity discharge and surface discharge. It is well known that a good database is an essential pre-requisite for developing a robust pattern classification system. Keeping this requirement in mind, experimentally gathered PD pattern data from two different measuring systems and recorded under different experimental conditions (in laboratories abroad, see acknowledgments) were pooled to form the database. Simple defect models were used in the experiments. Thus, the database included PD patterns acquired from two different detectors (namely a Haefely PD measuring system, TEAS 570, and a Tettex PD measuring system, Type 9126), recorded at different times, at different voltage levels, but arising basically due to a similar PD source. The PD patterns are stored as 256×256 and 200×200 matrices respectively by the two detectors. In this work, all patterns were resized to 256×256 and normalized, prior to processing. The original single source patterns were ~15 for each source. It is believed that a wider variety has been introduced by using such a database.

Using these single source patterns, multi-source PD patterns were artificially generated by digital superposition, followed by normalization. To generate partial and completely overlapping PD patterns, the individual pulse clusters of one source were shifted, if necessary, with due care exercised to incorporate realistic phase and magnitude positions (usually observed during practical PD measurements). The shift in magnitude direction was along the entire magnitude axis, while the phase shift was of the order of ±20°. In this way, multi-source PD patterns were generated. The multi-source PD patterns considered for classification are:

1. Case A: single point corona and cavity discharge.
2. Case B: single point corona and surface discharge.
3. Case C: cavity discharge and surface discharges.

Each of these patterns were decomposed to three levels, employing the Daubechies wavelet with 56 coefficients.

5 RESULTS AND DISCUSSION

5.1 FEATURE EXTRACTION

As explained in Section 3, the third level reconstructed H and V images (having a size of 256×256) of the superposed PD pattern represent salient features pertaining to the individual sources in a separable form, and also preserve the phase and the magnitude positions of the individual PD pulse clusters and their phase spreads. Therefore, for classification, these H and V images must be represented suitably. Formulation of a suitable feature vector was carried out by averaging the H and V images, both in the magnitude and phase directions. Averaging in the phase direction retains the magnitude information and

averaging in the magnitude direction retains information in the phase direction. The feature extraction procedure is summarized below and was performed for both the H and V images.

Magnitude averaging: Image pixels are averaged viewing from the phase axis. This averages magnitude information and retains phase information, which is vital for classification. With a view to preserve salient features, and at the same time, minimize the lengths of these vectors (1×256), different reductions were examined, and it was found that a length of fifty (1×50) was suitable, both in terms of achieving a reduction and for recognition purposes. The nearest-neighbor interpolation method (MATLAB image processing toolbox) was utilized for converting the (1×256) vector to a (1×50) vector.

Phase averaging: Averaging was performed viewing the image from the magnitude axis, *i.e.* phase values were averaged. These vectors contain the magnitude information only, which is important for classification, because in some cases, despite superposition of pulse clusters along phase axis, they are separable when viewed along the magnitude axis. These vectors were resized to a length of twenty five (1×25) for the same reason stated above.

The final feature vector was formulated by concatenating the averaged phase and magnitude vectors as follows: Let H_{50} and V_{50} be the magnitude averaged vectors, and H_{25} and V_{25} be the phase averaged vectors, then feature vector is $[H_{50}\ V_{50}\ H_{25}\ V_{25}]$, which is of length 150.

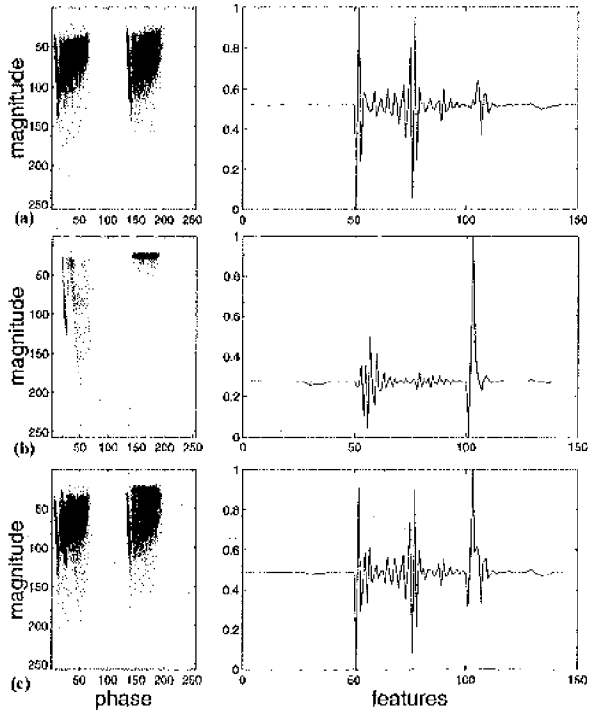

Figure 6. Feature vectors extracted for individual and superposed PD images in Figure 5(a), (d) and (g) respectively. (a) cavity discharge, (b) surface discharge, (c) (cavity + surface) discharge.

As an example, consider Figures 6(a) and (b) which shows the feature vectors for cavity discharge and surface discharge patterns (shown in Figure 5(a) and (d)) respectively. Figure 6(c) is the feature vector corresponding to the multi-source PD pattern (cavity and surface discharge) and shown in Figure 5(g). Figure 6(c) clearly indicates the separable form of the salient features present in the individual sources. Such a trend was observed in all the multi-source PD patterns examined. Next, these features are to be tested for their classification abilities. Figure 7 is a block diagram outlining the scheme of action.

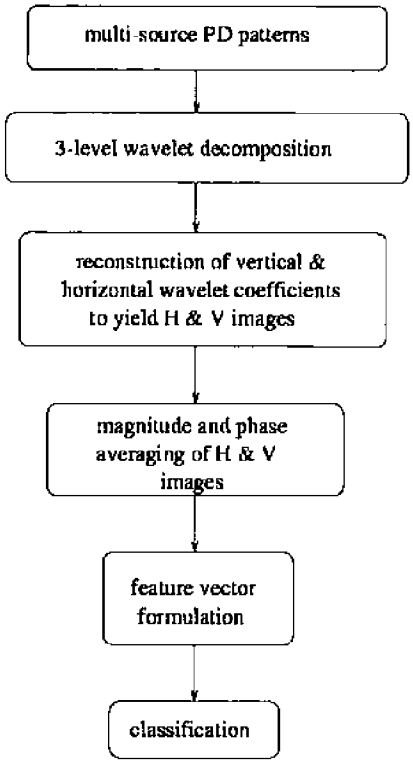

Figure 7. Scheme adopted for multi-source PD classification.

5.2 CLASSIFICATION

In this work, a neural network (NN) was utilized solely to illustrate the classification abilities of the features extracted. A NN is reported to be suitable for classification purposes due to its learning and generalization capabilities. In this work, the radial basis function NN was used. The advantage of this architecture is its evolving structure, in contrast to the backpropagation algorithm, where architecture *a priori* has to be fixed by trial and error. Learning in a radial basis function network is equivalent to finding a surface in a multi-dimensional space that provides a best fit to training data and generalization is equivalent to use of this multi-dimensional surface to interpolate the test data. It uses the Euclidean norm for the distance measure, instead of derivatives, as in backpropagation algorithm, and hence has faster convergence [14].

The number of input layer neurons were 150 (equal to length of the feature vector) and the output layer had three neurons (equal to the number of multi-source patterns considered). The training-set had 60 patterns, 20 for each type of two-source patterns considered. The convergence is considered to be achieved, when the overall sum-squared

Table 1. Classification results: the number of test patterns N and the number of correctly classified patterns P.

Case	N	P
A	150	130
B	73	65
C	90	81

error of the network was 0.001. This is the cumulative error for one epoch *i.e.* after all the training patterns are fed once. The number of epochs required for the convergence was observed to be 60, during different independent training sessions.

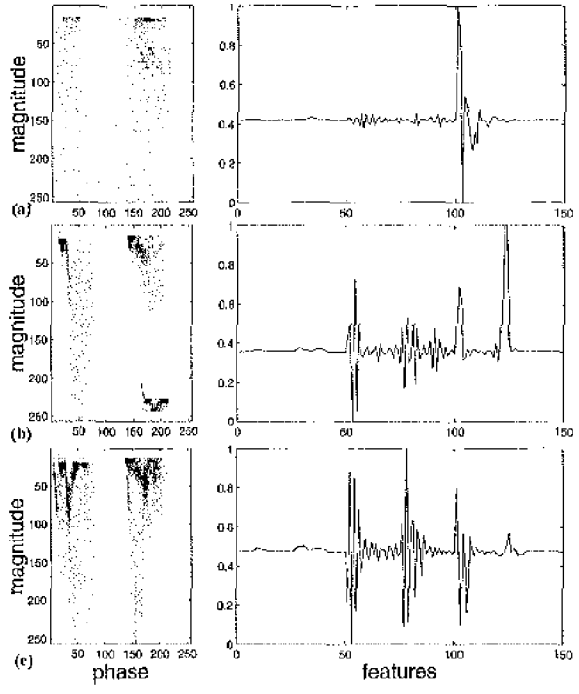

Figure 8. Example patterns of cases A, B and C that were correctly classified, along with their feature vectors.

To test the robustness of the features extracted, a certain amount of noise (~30%) and shift (as mentioned in Section 4), were added to the existing patterns and feature extraction was performed. These new features were then tested for classification, using the converged NN. Nearly, 100 patterns for each type of the multi-source PD (and those not included in the training-set) were tested. A majority of these testing patterns were either partially or fully overlapping PD patterns. When the output layer neurons yielded a value >0.6, it was considered as classified into that class. In all, correct classification was obtained for >88% of the patterns. As an example, Figure 8 illustrates multi-source PD patterns (one each from case A, B and C respectively), which have been correctly classified by the trained NN. Also shown are the corresponding feature vectors. The results are summarized in Table 1.

A few instances of misclassifications were also observed when the prominent features in H or V components in one of the sources were exactly similar in size and physical location of the second source, to which the first source was being added. Except for a few such extreme cases, more or less good recognition capabilities were achieved, thus, demonstrating the potential of this new method. A major contribution to the misclassfication were these multi-source patterns possessing excessive phase and magnitude shifts, for which the NN was not trained for.

Since, the primary aim was to demonstrate the principle of this method, to begin with, only three PD sources were examined. However, multi-source PD patterns generated from different individual sources, remain to be investigated, which will throw more light on the potential of this approach. To the question, as to how would the method behave, if more than two PD sources are present, a speculative answer would be that the feature vector will have to be more carefully formulated, so that it could capture faithfully the salient features of the sources present. Also, it is very likely that when more sources are present, the weaker ones will get swamped by the more powerful ones. This is a matter of concern and further research is necessary to find appropriate answers. However, when two sources are present, the feature vector is robust enough to take care of these artifacts.

6 CONCLUSIONS

THE multi-source PD recognition problem, usually encountered during practical PD measurements, is as yet an unresolved task, except in a few cases where the individual PD sources produce non-overlapping patterns. In this contribution, the novel use of MSD (a kind wavelet of transform) has been demonstrated to be suitable for this task, even in the presence of fully overlapping PD patterns. Employing the Daubechies wavelet, the multi-source PD pattern, treated as an image, was subjected to a three level decomposition and reconstruction process. The third level reconstructed horizontal (H) and vertical (V) component images were observed to contain the characteristic pattern features corresponding to the individual sources, and most importantly, in a separable form. Using these H and V images, suitable features were extracted, which were then tested for their classification abilities using the radial basis function NN. Results analyzed (after >300 partially and fully overlapping patterns were tested) seems to indicate the potential of this approach for this task. However, further study with different and actual multi-source PD patterns should be performed to reveal true capabilities and drawbacks, if any, of the proposed method.

ACKNOWLEDGMENT

The authors wish to express their thanks to E. Gulski of TU Delft, The Netherlands, for supplying some PD patterns that were used in an earlier joint contribution. Thanks are also due to Tettex Instruments AG, Deitikon, Switzerland, who have been kind to permit the use of some PD patterns, recorded by the second author some years earlier.

REFERENCES

[1] D. König and Y. Narayana Rao, *Partial Discharges in Electrical Power Apparatus*, VDE-verlag publishers, 1993.

[2] IEC Standard 60270, Partial Discharge Measurements, Committee Draft, IEC TC 42, WG 11, 39 IWD, Zaengl, Sept. 1995.

[3] E. Gulski and F. H. Kreuger, "Computer-aided Recognition of Discharge Sources", IEEE Transactions on Electrical Insulation, Vol. 27, No. 1, pp. 82–92, Feb. 1992.

[4] B. M. Lalitha and L. Satish, "Fractal Image Compression Technoque for Classification of PD Sources", IEEE Transactions on Dielectrics and Electrical Insulation, Vol. 5, No. 4, pp. 550–557, Aug 1998.

[5] June-Ho Lee, Doo-Sung Shin and T. Okamoto, "Analysis of Partial Discharge Signals from Multi-Defect Insulation Systems", Proc. of 4th International Conference on Properties and Applications of Dielectric Materials, May 25–30, 1997, Seoul, Korea.

[6] E. Binder, A. Draxler, H. Egger, A. Hummer, M. Muhr and G. Praxl, "Experience with on-line and off-line PD measurements of generators", CIGRE Session 1998, Paris, paper 15. 106.

[7] M. Cacciari and A. Contin, "Identification and Separation of Two Concurrent Partial Discharge Phenomena", Conference on Electrical Insulation and Dielectric Phenomena, San Fransisco, Oct. 20–23, 1996, pp. 476–479.

[8] June-Ho Lee, Doo-Sung Shin and Tatshuki Okamoto, "Analysis of Partial Discharge Signals from Multi-Defect Insulating Systems", Proc. of 5th Int. Conf. on Properties and Applications of Dielectric materials, May 25 -30, 1997, Seoul, Korea, pp. 307–310.

[9] J. S. Pearson, O. Farish, B. F. Hampton, M. D. Judd, D. Templeton, B. M. Pryor and J. M. Welch, "Partial Discharge Diagnostics for Gas Insulated Substations", IEEE Transactions on Dielectrics and Electrical Insulation, Vol. 2, No. 5, pp. 893–905, Oct. 1995.

[10] C. Cachin and H. J. Wiesmann, "PD Recognition with Knowledge-based Processing and Neural Networks", IEEE Transactons on Dielectrics and Electrical Insulation, Vol. 2, No. 4, pp. 578–589, Aug. 1995.

[11] A. Krivda and S. Halen, "Recognition of PD Patterns in Generators", Proc. of 5th Int. Conf. on Properties and Applications of Dielectric Materials, May 25–30, 1997, Seoul, Korea, pp. 206–211.

[12] Randy K. Young, *Wavelet theory and applications*, Kluwer Academic publishers, 1993.

[13] Y. Meyer (Editor), *Wavelets and Applications*, SpringerVerlag, 1989.

[14] Simon Haykins, *Neural Networks - a comprehensive foundation*, Macmillan publishers.

Manuscript was received on 12 December 1998, in revised form 19 November 1999.